

Harvesting entropy and quantifying the transition from noise to chaos in a photon-counting feedback loop

Aaron M. Hagerstrom, Thomas E. Murphy, Rajarshi Roy

June 14, 2022

Abstract

Some physical processes, including the intensity fluctuations of a chaotic laser, the detection of single photons, and the Brownian motion of a microscopic particle in a fluid are unpredictable, at least on long timescales. This unpredictability can be due to a variety of physical mechanisms, but it is quantified by an entropy rate. This rate describes how quickly a system produces new and random information, is fundamentally important in statistical mechanics and practically important for random number generation. We experimentally study entropy generation and the emergence of deterministic chaotic dynamics from discrete noise in a system that applies feedback to a weak optical signal at the single-photon level. We show that the dynamics qualitatively change from shot noise to chaos as the photon rate increases, and that the entropy rate can reflect either the deterministic or noisy aspects of the system depending on the sampling rate and resolution.

Continuous variables and dynamical equations are often used to model systems whose time evolution is comprised of discrete events occurring at random times. Examples include the flow of ions across cell membranes [1], the birth and death of individuals in a population [2], traffic flow on roads [3], the trading of securities in financial markets [4], infection and transmission of disease [5], and the emission and detection of photons [6]. We can identify two sources of unpredictability in these systems: the noise associated with the underlying random occurrences that comprise these signals, which is often described by a Poisson process, and the macroscopic dynamics of the system, which may be chaotic. When both effects are present, the macroscopic dynamics can alter the statistics of the noise, and the small-scale noise can in turn feed the large-scale dynamics. Dynamical unpredictability and complexity are quantified by Lyapunov exponents and dimensionality, while shot noise is characterized by statistical metrics like average rate, variance, and signal-to-noise ratio. Characterizing the unpredictability of a system with both large-scale dynamics and small-scale shot noise remains an important challenge in many disciplines including information security and statistical mechanics.

Many cryptographic applications, including public key encryption [7] employ random numbers. Because the unpredictability of these numbers is essential, physical processes are sometimes used as a source of random numbers [8–20]. The reliability of a physical random number generator depends on an accurate

assessment of the entropy rate of physical process that generated the numbers [21]. Evaluation of entropy rates is also centrally important in statistical mechanics in part because the relationship between information entropy, which measures unpredictability, and thermodynamic entropy, which is related to heat dissipation, is a fundamental issue [22–26]. One might expect that the unpredictability of a system with both small-scale shot noise and chaotic large-scale chaotic dynamics would depend on the scale at which it is observed. The unpredictability of physical systems across a range of scales has been studied both theoretically [27–30], and experimentally in Brownian motion and RC circuits [25, 26, 31].

Here, we present an experimental exploration of entropy production in a photon-counting optoelectronic feedback oscillator. Optoelectronic feedback loops which employ analog detectors and macroscopic optical signals produce rich dynamics whose timescales and dimensionality are highly tunable [32–36]. Our system applies optoelectronic feedback to a weak optical signal which is measured by a photon-counting detector. The dynamic range of this system (eight orders of magnitude in time scale and six orders of magnitude in photon counts) allows us to directly observe the transition from shot-noise dominated behavior to a low-dimensional chaotic attractor with increasing optical power. We show that the entropy rate can reflect either the deterministic or stochastic aspects of the system, depending on the sampling rate and measurement resolution.

Experimental system

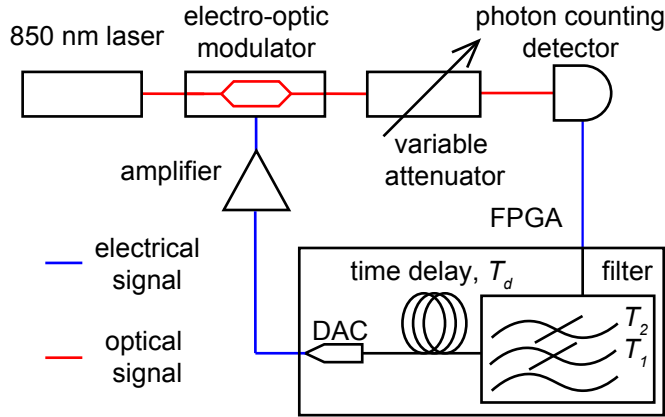


Figure 1: Experimental configuration. We employ an avalanche photodiode, which detects individual photon arrivals. This signal is time-delayed and filtered using an FPGA, and the output of the filter drives the modulator which in turn varies the light incident on the detector, forming a feedback loop.

Figure 1 shows a schematic of our experimental configuration. Our system has a similar architecture to earlier experiments involving optoelectronic feedback loops, but differs in that we use a photon-counting detector, whereas previous experiments used an analog photodetector. In either case, the signal

from the detector is time-delayed and filtered, and the output of the filter drives the Mach-Zehnder electro-optic modulator (MZM) which in turn controls the light incident on the detector, forming a feedback loop. When an analog photodiode is used, the feedback loop is modeled a time-delayed nonlinear differential equation.

$$\begin{aligned}\frac{d\mathbf{x}}{dt} &= \mathbf{E}\mathbf{x} + \beta\mathbf{F}I(t) \\ I(t) &= \sin^2 [\mathbf{G}^T \mathbf{x}(t - T_d) + \phi]\end{aligned}\quad (1)$$

Here, \mathbf{x} is the state variable of a linear, time invariant filter, matrix \mathbf{E} and the vectors \mathbf{F} and \mathbf{G} describe the characteristics of the filter, $I(t)$ is the normalized intensity of light transmitted through the MZM, and T_d is the time delay. When a photon-counting detector is used in place of an analog photodiode, the filter variables can be modeled by a linear differential equation driven by discrete photon arrivals. In our implementation, the equations of motion for the filter variables are

$$\frac{d}{dt} \begin{pmatrix} x_1 \\ x_2 \end{pmatrix} = \begin{pmatrix} -\frac{1}{T_1} & 0 \\ 0 & -\frac{1}{T_2} \end{pmatrix} \begin{pmatrix} x_1 \\ x_2 \end{pmatrix} + \beta \begin{pmatrix} 1 \\ 1 \end{pmatrix} \frac{1}{\lambda_0} \sum_{i=1}^{\infty} \delta(t - t_i), \quad (2)$$

where the photon arrivals times, $\{t_i\}$, are generated by an non-stationary Poisson point process whose rate, $\lambda(t)$, depends on the state of the filter variables.

$$\lambda(t) = \lambda_0 I(t) = \lambda_0 \sin^2 [x_1(t - T_d) - x_2(t - T_d) + \phi]. \quad (3)$$

In the limit that the λ_0 is large, the stochastic term in equation (2) can be replaced with its expectation value, $I(t)$, leading to equation (1).

In our implementation, the time delay is $T_d=1.734$ ms, the modulator bias is $\phi = \pi/4$, and the filter constants $T_1=1.2$ ms, and $T_2=60$ μ s. The filter and time delay are implemented digitally using an Altera Cyclone II field programmable gate array (FPGA) and a digital to analog converter (DAC). The clock speed of this device is 151.1515 MHz, and we record all of the photon arrival times to this precision. The light source in our experiment is a continuous wave fiber-coupled distributed feedback laser with a wavelength of 850 nm. Our detector has a dark count rate of ~ 100 counts/s and a dead time of about 100 ns. We vary the photon rate over a factor of 256, from $\lambda_0 T_d = 12.5$ (7.20×10^3 count/s) to $\lambda_0 T_d = 3200$ (1.845×10^6 counts/s). In all of the experiments shown here, β is kept constant at 8.87.

Noise and complex dynamics in a photon-counting feedback loop

Figure 2 shows several time series recorded with this system with increasing photon rate, showing a transition from Poisson noise to deterministic chaos. We plot $N_w(t)$, the number of photon arrivals in the interval $[t - w, t]$. In Figure 2, all of the plots were generated with $w = T_d/4$. When the incident photon rate is $\lambda_0 T_d = 12.5$, the photons appear to arrive at random, uncorrelated times as in a stationary Poisson process. Increasing the incident photon rate to $\lambda_0 T_d = 200$, a smooth modulation of the photon rate starts to become apparent. At $\lambda_0 T_d = 3200$, $N_w(t)$ has a smooth character, and qualitatively resembles a

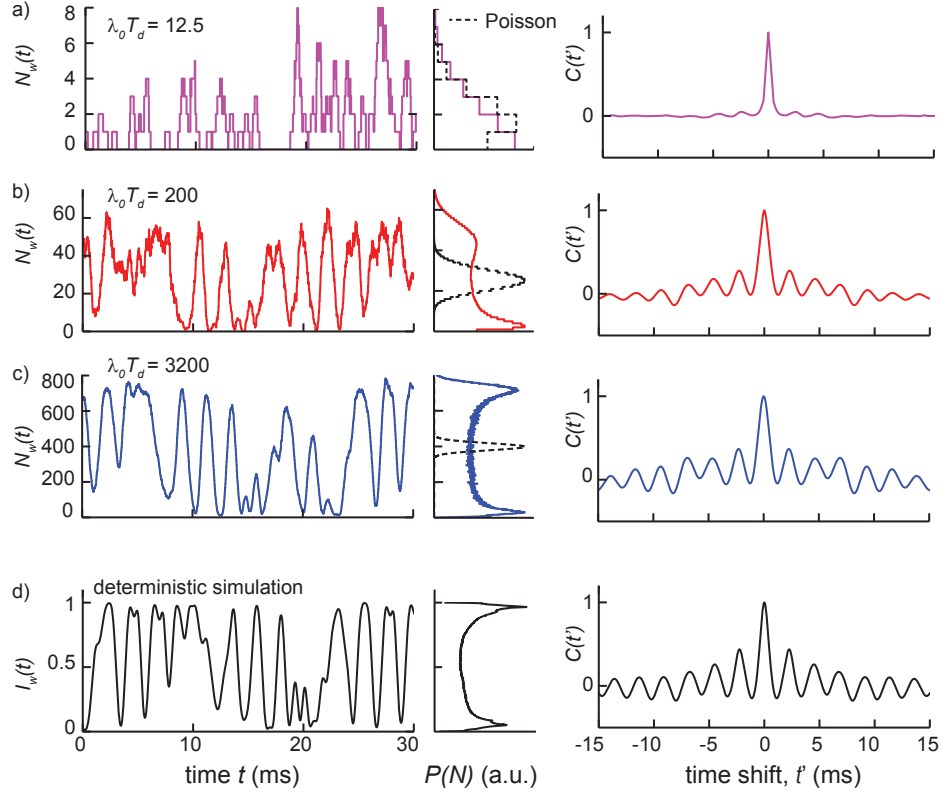


Figure 2: Time series, probability distributions, and autocorrelation functions. a) - c) show experimental data, and d) shows the result of a deterministic simulation of Equation (1). a) At a low photon rate of $\lambda_0 T_d = 12.5$, the dynamics appear Poissonian. The time series has no visible structure, the autocorrelation function is sharply peaked at 0, and the distribution of photon counts in a window of $w = T_d/4$ is nearly Poisson. b) $\lambda_0 T_d = 200$, a slow modulation of the photon rate is evident. c) at $\lambda_0 T_d = 3200$, the photon rate varies smoothly, the photon count distribution is bimodal and much wider than a Poisson distribution with the same mean, and the autocorrelation function shows slow oscillations. The deterministic simulation d) shows the same features as the high photon rate data shown in c).

low-dimensional chaotic signal. We also plot the results of a deterministic simulation using equation (1). This time series was smoothed with a moving average over a time window of width w to be directly comparable with $N_w(t)$. We plot the autocorrelation function, $C(t') = \langle (N_w(t) - \bar{N}_w)(N_w(t - t') - \bar{N}_w) \rangle$, normalized so that the value of the autocorrelation function is unity at $t' = 0$. As the photon rate increases from $\lambda_0 T_d = 12.5$, the autocorrelation function changes from a δ -like peak, characteristic of a Poisson process, to an oscillatory function which shows correlations at long timescales (tens of milliseconds). The autocorrelation function of the deterministic simulation time series is in close agreement with the autocorrelation function of the photon arrivals with $\lambda_0 T_d = 3200$. Histograms of $N_w(t)$ also show a transition from a nearly Poisson distribution to a bimodal distribution characteristic of the deterministic chaotic process.

To visualize the development of chaos with increasing photon rate, we show Poincaré surfaces of section in Figure 3. We perform a time-delay embedding of the experimental time series $N_w(t)$, using a time delay of $\Delta = T_d/4$, by constructing a list of points in two dimensional space of the form $[N_w(t), N_w(t - \Delta)]$. Because the attractor has a dimension higher than 2, we reduce the dimensionality of the attractor by plotting the points only when the state variables pass through a codimension 1 Poincaré surface defined by $x_1 - x_2 = \pi$. The embeddings show a similar trend to the plots in Figure 2. We see a development of complex chaotic dynamics from discrete photon noise as the photon rate increases. The deterministic simulation is plotted for comparison, and, as in Figure 2, a moving average of width w is employed so that the smoothed intensity time series, $I_w(t)$, is directly analogous to $N_w(t)$. The deterministic signal in Figure 3d can be regarded as the infinite photon rate limit of the photon counting system.

Figure 4 shows the dependence of the variance of N_w on the window w and offers another indication of the transition from shot noise to deterministic chaos. The time integral of an uncorrelated random signal executes a random walk in which the variance grows linearly with the integration time. For this reason, we plot $\text{Var}(N_w)/w$ in Figure 4. We see distinct asymptotic growth rates of the variance with small and large w . When w is small, the variance reflects the Poissonian nature of the photon arrivals, and the growth rate of the variance has roughly constant value of $\text{Var}(N_w)/w = \lambda_0 \bar{I}$. In the limit where the counting window is much longer than the time scale the variations in intensity, $N_w(t)$ can be regarded as the sum of the photon counts in many independent identically distributed intervals, and the central limit theorem implies that the variance will grow in proportion to w . As we increase the photon rate from $\lambda_0 T_d = 12.5$ to $\lambda_0 T_d = 3200$, we see an increasing offset between the two asymptotic rates of growth of the variance. The variance can be related to the photon rate, counting window, and the unnormalized autocorrelation function, $c_I(t') = \langle (I(t) - \bar{I})(I(t - t') - \bar{I}) \rangle$ [6].

$$\text{Var}(N_w) = w \left[\lambda_0 \bar{I} + \underbrace{\lambda_0^2 \int_{-w}^w dt' \left(1 - \frac{|t'|}{w} \right) c_I(t')}_{\Theta(w)} \right] \quad (4)$$

The second term in Equation (4) accounts for the difference between the ob-

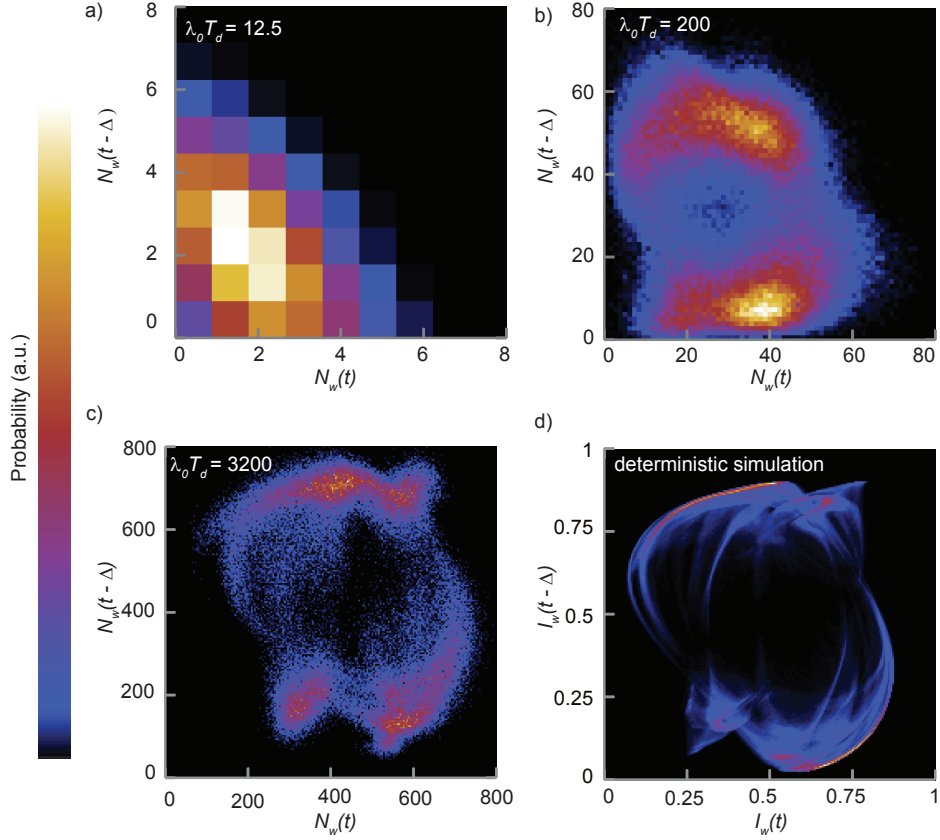


Figure 3: Poincaré sections. We visualize the emergence of a low-dimensional chaotic attractor from Poisson noise with increasing photon rate by embedding photon count time series in two dimensions with a time delay of $\Delta = T_d/4$, and reducing the dimensionality of the dynamics by plotting points only when the state of the system in phase space passes through a codimension-1 surface defined by $x_1 - x_2 = \pi$. a) - c) show experimental data, and d) shows the result of a deterministic simulation. These histograms are constructed with a bin width of 1 photon in a) and b), 4 photons in c), and 0.005 in d)

served variance and the variance of a Poisson process with the same rate. The quantity $\Theta(w)$ has units of time, and measures the correlations in $I(t)$ introduced by the feedback. This quantity increases from 0 to an asymptotic value Θ_∞ as w increases, accounting for the shape of the curves shown in Figure 4. In deterministic simulations, we find $\Theta_\infty = 150 \mu\text{s}$. The value of Θ_∞ is related to the size of the intensity fluctuations, and the rate at which $\Theta(w)$ approaches this asymptotic value is determined by the timescales of the correlations of $I(t)$.

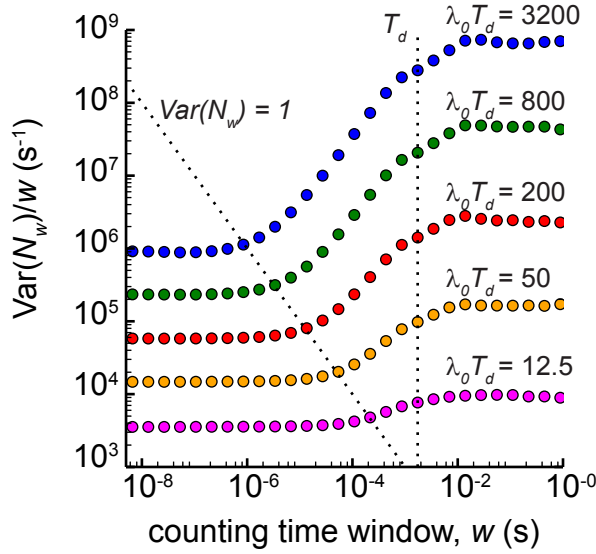


Figure 4: Experimental dependence of growth rate of variance on counting time window, w . To indicate the timescale of the deterministic dynamics we indicate T_d . We also show a line indicating $\text{Var}(N_w) = 1$, which roughly separates timescales over which less than one photon arrives from timescales over which many photons arrive. Distinct asymptotic values of $\text{Var}(N_w)/w$ are seen in the limits of small and large w . The offset between these two values reflects deterministic correlations in the photon arrival rate and grows with increasing photon rate.

Entropy production

We characterize the entropy production using the (ε, τ) entropy per unit time, $h(\varepsilon, \tau)$ [27]. This measurement of entropy has two parameters: sample resolution, ε , and sampling time interval τ , which are natural parameters for most experiments because measurement devices record data to finite resolution at discrete times. In addition to being experimentally relevant, the dependence of $h(\varepsilon, \tau)$ on these parameters can reflect the underlying physical origin of unpredictability [27, 29, 30].

In chaotic systems, unpredictability is due to the sensitive dependence on initial conditions. Because small perturbations grow exponentially in time, chaotic systems generate information. The growth of uncertainty is quantified by the Lyapunov exponents μ_i , and in particular the largest exponent, μ_1 . Positive Lyapunov exponents and entropy rate both quantify unpredictability and there is a close relationship between these two quantities. One would expect that if a chaotic system is sampled infrequently ($\tau\mu_1 \gg 1$), successive samples will be uncorrelated because of the growth of uncertainty between measurements. On the other hand, if the interval between successive samples is small ($\tau\mu_1 \ll 1$), one expects strong correlations between adjacent samples and a reduced entropy per sample. Experimental and theoretical work using semiconductor lasers has shown that these considerations are crucial to physical random number generation using chaotic dynamics [15,16,37]. In the limit that $\tau, \varepsilon \rightarrow 0$, $h(\varepsilon, \tau)$ will approach a finite value, the Kolmogorov-Sinai (or metric) entropy, h_{ks} [30,38–40]. The metric entropy is related to the Lyapunov exponents, μ_i , by

$$h_{ks} = \frac{1}{\log(2)} \sum_{\mu_i > 0} \mu_i. \quad (5)$$

We calculated the spectrum of Lyapunov exponents from Equation (1) [41,42]. There is only one positive Lyapunov exponent with a value of $\mu_1/\log(2) = 345$ bits/s. The Kaplan-Yorke dimension [43] calculated from the Lyapunov spectrum is 3.56, consistent with the visual appearance of Figure 3.

The (ε, τ) entropy will have qualitatively different behavior as $\varepsilon \rightarrow 0$ depending on the physical origin of unpredictability. In chaotic systems, the entropy rate does not depend on either the sampling rate or the sampling resolution. This property of chaotic systems imposes a theoretical limitation on physical random number generation. Increasing the speed and resolution of a measurement device cannot in principle increase the entropy that can be harvested from a deterministic chaotic system beyond h_{ks} . In contrast to deterministic systems, the entropy rate of stochastic signals diverges like $-\log(\varepsilon)$ for finite τ [27,29].

Another advantage of the (ε, τ) entropy is that it can be calculated from experimental data using an algorithm described by Cohen and Procaccia [44]. In our case, we chose to calculate the entropy from $N_w(t)$ with a counting time window of $w = T_d/4$. With this window, $N_w(t)$ approximates the behavior of the deterministic signal $I(t)$ as seen in Figures 2 and 3. We do not employ an averaging time window to compute the entropy from deterministic simulations.

The first step to computing the entropy rate of an experimental signal is to generate list of points in d -dimensional space using time delay embedding with a delay of τ . These vectors can be regarded as samples of a d -dimensional probability distribution over phase space. The entropy of this probability distribution, H_d , is sometimes referred to as the pattern entropy for patterns of length d [31]. In principle H_d can be calculated by building a histogram with boxes of width ε and applying Shannon’s formula, $H = -\sum_i p_i \log_2 p_i$ [45]. In practice, direct application of this approach requires a very large amount of data when the embedding dimension is large. Cohen and Procaccia proposed a more efficient algorithm to estimate the pattern entropy [44] in the context of estimating metric entropy from experimental data. First, one randomly selects a small number M of reference points from the time series. In our case,

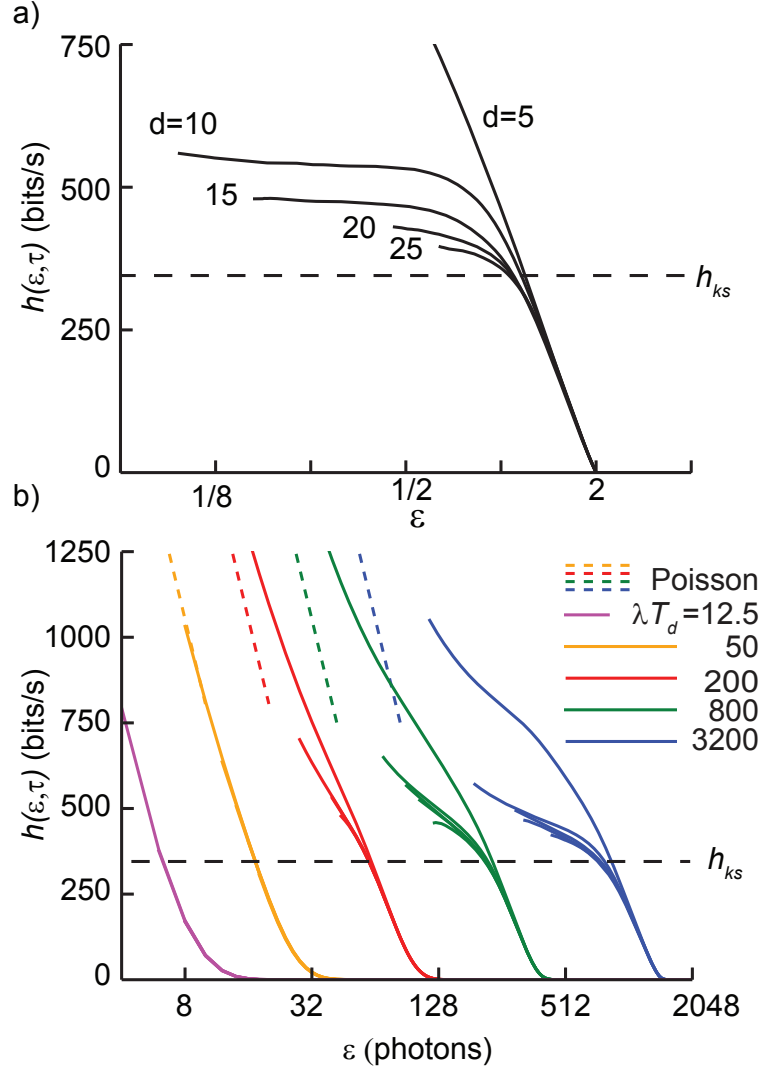


Figure 5: (ε, τ) entropy in deterministic simulation and experiment. Calculations with embedding dimensions of 5, 10, 15, 20 and 25 are shown. a) deterministic simulation. Characteristic of deterministic systems, the entropy rate is independent of ε , and approaches the largest Lyapunov exponent as d increase. b) Entropy rate of experimental time series. The entropy rate flattens and approaches h_{ks} as the photon rate increases. At high photon rates and small ε , we see a divergence characteristic of a Poisson processes. The Poisson curves were calculated by approximating the Shannon entropy of a Poisson process by an integral over a Gaussian distribution with a mean and variance of $\lambda_0 \bar{I} w$.

$M = 5000$ was sufficient. For each reference point i , one computes $n_i(\varepsilon)$, the fraction of points within a box of width ε centered on the reference point. The only difference between a direct calculation of the Shannon entropy, and the Cohen-Procaccia procedure is that in a direct calculation, a rectangular array of bins is used, rather than a set of bins centered on random points chosen from the data set. In searching for neighbors for the i th reference point, we exclude points within a time window of τ of that point, as suggested by Theiler [46]. The pattern entropy is then estimated by

$$H_d(\varepsilon) = -\frac{1}{M} \sum_{i=1}^M \log_2 n_i(\varepsilon). \quad (6)$$

It is a general feature of unpredictable signals that H_d grows linearly with d in the limit that d is large, and the entropy rate is the slope of this linear increase.

$$h(\varepsilon, \tau) = \frac{1}{\tau} \lim_{d \rightarrow \infty} [H_d(\varepsilon) - H_{d-1}(\varepsilon)] \quad (7)$$

Figure 5 shows the entropy per unit time in both deterministic simulation and experiment with $\tau = (3/4)T_d$. Figure 5a shows that in the deterministic simulation, the entropy rate remains flat as ε decreases. As d increases, this plateau approaches h_{ks} , as indicated by Equation (5). A similar behavior is seen in the experimental system at a photon rate of $\lambda_0 T_d = 3200$ in Figure 5b, where we see a flattening of the curve at high ε . Furthermore, in the region that this flattening is present, the value of $h(\varepsilon, \tau)$ is close to h_{ks} . The flattening of $h(\varepsilon, \tau)$ at high photon rate is another indication that this system behaves more deterministically in this regime. At all photon rates, we see $h(\varepsilon, \tau)$ diverges as $-\log(\varepsilon)$, for small ε , which is due to the shot noise inherent in the system. It is natural to compare the entropy rates we observe to a constant-rate Poisson process with the same average rate. The Poisson curves in Figure 5 were calculated by approximating the Shannon entropy of a Poisson distribution by an integral over a Gaussian distribution with a mean and variance of $\lambda_0 \bar{I} w$. We see $h(\varepsilon, \tau)$ approach this approximate curve when ε and λ_0 are both small.

We show in this paper that the choice of the resolution with which we observe our system allows us to see either noisy or deterministic dynamics. By counting photon arrivals over timescales on the order of the delay time and filter time constants, we see deterministic dynamics in the appearance of the time series, Poincaré sections, and the autocorrelation functions. Furthermore, when we observe the dynamics on large scales of both value (ε) and time (w and τ), we find that the entropy rate is close in value to the metric entropy calculated from the positive Lyapunov exponents of the deterministic system. This shows that the entropy generation is dominated by the deterministic exponential amplification of small perturbations in this regime. In contrast, by employing high resolution in photon counts and time scales, we see that both the entropy rate and variance reflect the stochastic nature of the photon arrivals. For small values of w , the variance of the number of photon counts is equal to the average number of counts, characteristic of a Poisson process. The $-\log(\varepsilon)$ dependence of the entropy shown in Figure 5 offers another indication of the noisy nature of the dynamics at small scales. Our results have immediate relevance to physical random number generation, as they offer insight into how to determine how much entropy one is entitled to harvest from a physical

system, and how this quantity depends on the bandwidth and resolution of the measurement device. In addition to showing both shot noise and chaos at different scales, our experiment also shows a transition from shot noise to chaos with increasing photon rate. Our experimental system allows for both detailed observation over a range of scales in time and photon number as well as precise control over rate of photon arrivals and the timescales and dimensionality of the chaotic dynamics.

References

- [1] James Keener and James Sneyd. *Mathematical physiology: I: cellular physiology*, volume 1. Springer Science & Business Media, 2010.
- [2] Robert McCredie May. *Stability and complexity in model ecosystems*, volume 6. Princeton University Press, 2001.
- [3] Debashish Chowdhury, Ludger Santen, and Andreas Schadschneider. Statistical physics of vehicular traffic and some related systems. *Physics Reports*, 329(4):199–329, 2000.
- [4] Rosario N Mantegna and H Eugene Stanley. *Introduction to econophysics: correlations and complexity in finance*. Cambridge University Press, 1999.
- [5] Roy M Anderson and Robert McCredie May. *Infectious diseases of humans*, volume 1. Oxford University Press Oxford, 1991.
- [6] Leonard Mandel and Emil Wolf. *Optical coherence and quantum optics*. 1995. Equation (4) is found in section 14.9.2.
- [7] Arjen Lenstra, James P Hughes, Maxime Augier, Joppe Willem Bos, Thorsten Kleinjung, and Christophe Wachter. Ron was wrong, Whit is right. Technical report, IACR, 2012.
- [8] Mike Hamburg, Paul Kocher, and Mark E Marson. Analysis of intel’s ivy bridge digital random number generator. *Online: http://www.cryptography.com/public/pdf/Intel_TRN_G_Report_20120312.pdf*, 2012.
- [9] Taiki Yamazaki and Atsushi Uchida. Performance of random number generators using noise-based superluminescent diode and chaos-based semiconductor lasers. *IEEE Journal of Selected Topics in Quantum Electronics*, 19(4):0600309–0600309, 2013.
- [10] Ryohsuke Sakuraba, Kento Iwakawa, Kazutaka Kanno, and Atsushi Uchida. Tb/s physical random bit generation with bandwidth-enhanced chaos in three-cascaded semiconductor lasers. *Optics Express*, 23(2):1470–1490, 2015.
- [11] Xiaowen Li, Adam B. Cohen, Thomas E. Murphy, and Rajarshi Roy. Scalable parallel physical random number generator based on a superluminescent LED. *Opt. Lett.*, 36(6):1020–1022, Mar 2011.
- [12] Caitlin R. S. Williams, Julia C. Salevan, Xiaowen Li, Rajarshi Roy, and Thomas E. Murphy. Fast physical random number generator using amplified spontaneous emission. *Opt. Express*, 18(23):23584–23597, Nov 2010.

- [13] David P. Rosin, Damien Rontani, and Daniel J. Gauthier. Ultrafast physical generation of random numbers using hybrid Boolean networks. *Physical Review E*, 87:040902, Apr 2013.
- [14] Ido Kanter, Yaara Aviad, Igor Reidler, Elad Cohen, and Michael Rosenbluh. An optical ultrafast random bit generator. *Nature Photonics*, 4(1):58–61, 2009.
- [15] Takahisa Harayama, Satoshi Sunada, Kazuyuki Yoshimura, Jun Muramatsu, Ken-ichi Arai, Atsushi Uchida, and Peter Davis. Theory of fast nondeterministic physical random-bit generation with chaotic lasers. *Physical Review E*, 85:046215, Apr 2012.
- [16] Satoshi Sunada, Takahisa Harayama, Peter Davis, Ken Tsuzuki, Ken-ichi Arai, Kazuyuki Yoshimura, and Atsushi Uchida. Noise amplification by chaotic dynamics in a delayed feedback laser system and its application to nondeterministic random bit generation. *Chaos: An Interdisciplinary Journal of Nonlinear Science*, 22(4):047513, 2012.
- [17] Neus Oliver, Miguel C. Soriano, David W. Sukow, and Ingo Fischer. Dynamics of a semiconductor laser with polarization-rotated feedback and its utilization for random bit generation. *Opt. Lett.*, 36(23):4632–4634, Dec 2011.
- [18] Neus Oliver, Miguel Cornelles Soriano, David W Sukow, and Ingo Fischer. Fast random bit generation using a chaotic laser: approaching the information theoretic limit. *Quantum Electronics, IEEE Journal of*, 49(11):910–918, 2013.
- [19] Martin Virte, Emeric Mercier, Hugo Thienpont, Krassimir Panajotov, and Marc Sciamanna. Physical random bit generation from chaotic solitary laser diode. *Optics Express*, 22(14):17271–17280, 2014.
- [20] Christian Gabriel, Christoffer Wittmann, Denis Sych, Ruifang Dong, Wolfgang Mauere, Ulrik L. Andersen, Christoph Marquardt, and Gerd Leuchs. A generator for unique quantum random numbers based on vacuum states. *Nature Photonics*, 4(10):711–715, 2010.
- [21] Elaine Barker and John Kelsey. NIST DRAFT Special Publication 800-90b recommendation for the entropy sources used for random bit generation. 2012.
- [22] Christopher Jarzynski. Diverse phenomena, common themes. *Nature Physics*, 11(2):105–107, 2015.
- [23] Hugo Touchette. The large deviation approach to statistical mechanics. *Physics Reports*, 478(1):1–69, 2009.
- [24] Édgar Roldán and Juan M. R. Parrondo. Estimating Dissipation from Single Stationary Trajectories. *Phys. Rev. Lett.*, 105:150607, Oct 2010.
- [25] David Andrieux, Pierre Gaspard, Sergio Ciliberto, Nicolas Garnier, Sylvain Joubaud, and Artyom Petrosyan. Entropy production and time asymmetry in nonequilibrium fluctuations. *Physical Review Letters*, 98(15):150601, 2007.

- [26] D. Andrieux, P. Gaspard, S. Ciliberto, N. Garnier, S. Joubaud, and A. Petrosyan. Thermodynamic time asymmetry in non-equilibrium fluctuations. *Journal of Statistical Mechanics: Theory and Experiment*, 2008(01):P01002, 2008.
- [27] Pierre Gaspard and Xiao-Jing Wang. Noise, chaos, and (ε, τ) -entropy per unit time. *Physics Reports*, 235(6):291–343, 1993.
- [28] C.P. Dettmann, E.G.D. Cohen, and Van Beijeren H. Statistical mechanics: Microscopic chaos from Brownian motion? *Nature*, 401(6756):875–875, 1999.
- [29] M Cencini, M Falcioni, E Olbrich, H Kantz, and A Vulpiani. Chaos or noise: Difficulties of a distinction. *Physical Review E*, 62(1):427, 2000.
- [30] Guido Boffetta, Massimo Cencini, Massimo Falcioni, and Angelo Vulpiani. Predictability: a way to characterize complexity. *Physics Reports*, 356(6):367–474, 2002.
- [31] P. Gaspard, M.E. Briggs, M.K. Francis, J.V. Sengers, R.W. Gammon, J.R. Dorfman, and R.V. Calabrese. Experimental evidence for microscopic chaos. *Nature*, 394(6696):865–868, 1998.
- [32] Michael Peil, Maxime Jacquot, Yanne Kouomou Chembo, Laurent Larger, and Thomas Erneux. Routes to chaos and multiple time scale dynamics in broadband bandpass nonlinear delay electro-optic oscillators. *Physical Review E*, 79:026208, Feb 2009.
- [33] Thomas E. Murphy, Adam B. Cohen, Bhargava Ravoori, Karl R.B. Schmitt, Anurag V. Setty, Francesco Sorrentino, Caitlin R.S. Williams, Edward Ott, and Rajarshi Roy. Complex dynamics and synchronization of delayed-feedback nonlinear oscillators. *Philosophical Transactions of the Royal Society A: Mathematical, Physical and Engineering Sciences*, 368(1911):343–366, 2010.
- [34] Laurent Larger. Complexity in electro-optic delay dynamics: modelling, design and applications. *Philosophical Transactions of the Royal Society A: Mathematical, Physical and Engineering Sciences*, 371(1999), 2013.
- [35] Caitlin R. S. Williams, Thomas E. Murphy, Rajarshi Roy, Francesco Sorrentino, Thomas Dahms, and Eckehard Schöll. Experimental Observations of Group Synchrony in a System of Chaotic Optoelectronic Oscillators. *Phys. Rev. Lett.*, 110:064104, Feb 2013.
- [36] Y. Chembo Kouomou, Pere Colet, Laurent Larger, and Nicolas Gastaud. Chaotic Breathers in Delayed Electro-Optical Systems. *Physical Review Letters*, 95:203903, Nov 2005.
- [37] Takuya Mikami, Kazutaka Kanno, Kota Aoyama, Atsushi Uchida, Tohru Ikeguchi, Takahisa Harayama, Satoshi Sunada, Ken-ichi Arai, Kazuyuki Yoshimura, and Peter Davis. Estimation of entropy rate in a fast physical random-bit generator using a chaotic semiconductor laser with intrinsic noise. *Physical Review E*, 85(1):016211, 2012.

- [38] Yakov Borisovich Pesin. Characteristic Lyapunov exponents and smooth ergodic theory. *Russian Mathematical Surveys*, 32(4):55–114, 1977.
- [39] J.-P. Eckmann and D. Ruelle. Ergodic theory of chaos and strange attractors. *Reviews of Modern Physics*, 57(3):617, 1985.
- [40] Giancarlo Benettin, Luigi Galgani, and Jean-Marie Strelcyn. Kolmogorov entropy and numerical experiments. *Physical Review A*, 14(6):2338, 1976.
- [41] J Doyne Farmer. Chaotic attractors of an infinite-dimensional dynamical system. *Physica D: Nonlinear Phenomena*, 4(3):366–393, 1982.
- [42] Karlheinz Geist, Ulrich Parlitz, and Werner Lauterborn. Comparison of different methods for computing Lyapunov exponents. *Progress of Theoretical Physics*, 83(5):875–893, 1990.
- [43] Peter Grassberger and Itamar Procaccia. Measuring the strangeness of strange attractors. *Physica D*, 9:189–208, 1983.
- [44] Aviad Cohen and Itamar Procaccia. Computing the Kolmogorov entropy from time signals of dissipative and conservative dynamical systems. *Phys. Rev. A*, 31:1872–1882, Mar 1985.
- [45] Thomas M Cover and Joy A Thomas. *Elements of information theory*. 2012. Chapter 4.
- [46] James Theiler. Estimating fractal dimension. *JOSA A*, 7(6):1055–1073, 1990.